Journal of Molecular Liquids 151 (2010) 30–38

Contents lists available at ScienceDirect

Journal of Molecular Liquids

journal homepage: www.elsevier.com/locate/molliq

Synthesis, characterization and mesomorphic properties of new unsymmetrical azomethine-type liquid crystals derived from 4-biphenyl carboxaldehyde

Agnieszka Iwan [a,*], Henryk Janeczek [b], Marian Domanski [b], Patrice Rannou [c]

[a] Electrotechnical Institute, Division of Electrotechnology and Materials Science, M. Sklodowskiej-Curie 55/61 Street, 50-369 Wroclaw, Poland
[b] Centre of Polymer and Carbon Materials, Polish Academy of Sciences, 34 M. Curie-Sklodowska Street, 41-819 Zabrze, Poland
[c] Laboratoire d'Electronique Moléculaire, Organique et Hybride, UMR5819-SPrAM (CEA-CNRS-Univ. J. FOURIER-Grenoble I),
INAC Institut Nanosciences & Cryogénie, CEA-Grenoble, 17 Rue des Martyrs, 38054 Grenoble Cedex 9, France

ARTICLE INFO

Article history:
Received 24 September 2009
Accepted 27 October 2009
Available online 4 November 2009

Keywords:
Azomethines
Imines
Liquid crystals
Mesomorphic behavior

ABSTRACT

Synthesis, characterization and thermal properties of a series of four azomethines (**1**)–(**4**) derived from 4-biphenyl carboxaldehyde were described. The structures of the azomethines were characterized by means FTIR, ^{1}H, ^{13}C NMR spectroscopy and elemental analysis; the results show an agreement with the proposed structure. The methods of differential scanning calorimetry (DSC) and polarizing optical microscopy (POM) were used to describe the liquid-crystalline properties of the azomethines. The mesomorphic properties of the compounds depend on the amine used in the synthesis of imines. In particular, three of them prepared from 4-hexadecylaniline, 4-decylaniline or 4-((4-aminophenyl)diazenyl)-N,N-dimethylbenzenamine (**1**)–(**3**) showed smectic A and smectic X mesophases, while the last one obtained from 4-(heptadecafluoroctyl)aniline (**4**) exhibited SmX2 and nematic mesophases. Current–voltage measurements were performed on ITO/compound/Alq$_3$/Al device with two different thicknesses of the film. Additionally, we compared the mesomorphic behavior of the azomethines presented in this work with another azomethines.

1. Introduction

Synthesis and thermal characterizations of new mesogens are one of the important areas for materials research community. A lot of compounds, polymers and dendrimers with different shapes, symmetries and consequently with different types of mesogens are synthesized and investigated as liquid-crystalline materials [1–13]. Among new mesogens, azomethines have a special interest [14]. These compounds exhibit dependently from the structure mono- or polymorphism and are very sensitive to different acids and have photochromic properties [14]. Additionally, these compounds are thermostable and create complexes with different types of metals [14]. Therefore these mesogenic compounds are very perspective materials for technical and technological applications.

The azomethines that exhibited different liquid-crystalline properties depend from the numbers of HC=N bonds in the structure. For this reason we could divide symmetrical and unsymmetrical azomethines for: (a) azomethines having one azomethine (HC=N) bond [15–23] and (b) azomethines with two HC=N bonds in the structure [24–34].

Here we presented a series of unsymmetrical azomethines with different end-groups and their thermal properties. The transition temperatures were studied by DSC and POM techniques. Current–voltage measurements were performed on ITO/compound/Alq$_3$/Al device.

Additionally, the aim of the paper was a comparison of the thermal properties of: (i) two azomethines obtained from 4-(heptadecafluoroctyl)aniline and two different aldehydes such as 4-biphenyl carboxaldehyde and 4-octadecyloxybenzaldehyde (compare (**3**) and (**A3**)) and (ii) four azomethines obtained from 4-((4-aminophenyl)diazenyl)-N,N-dimethylbenzenamine and 4-hexadecylaniline and two different aldehydes such as 4-(4,4,5,5,6,6,7,7,8,8,9,9,10,10,11,11,11-heptadecafluoroundecyloxy)benzaldehyde and 4-biphenyl carboxaldehyde (compare (**2**) and (**F2**) and (**4**) and (**F4**)).

2. Experimental section

2.1. Materials

Acetone, ethanol, N,N-dimethylacetamide (DMA) (Aldrich) and 4-biphenyl carboxaldehyde (Aldrich), 4-hexadecylaniline (Aldrich), 4-decylaniline (Aldrich), 4-((4-aminophenyl)diazenyl)-N,N-dimethylbenzenamine (Aldrich) and 4-(heptadecafluoroctyl)aniline (Fluka) were used without any purification.

2.2. Characterization techniques

All synthesized compounds were characterized by NMR and FTIR spectroscopy. NMR was recorded on a Bruker AC 200 MHz. Chloroform-*d*

---

[*] Corresponding author.
E-mail address: a.iwan@iel.wroc.pl (A. Iwan).

0167-7322/$ – see front matter © 2009 Elsevier B.V. All rights reserved.
doi:10.1016/j.molliq.2009.10.015

($CDCl_3$) containing TMS as an internal standard were used as solvent. FTIR spectra of the compounds were recorded on a Perkin-Elmer paragon 500 spectrometer (wavenumber range: 400–4000 cm^{-1}; resolution: 2 cm^{-1}). Current–voltage measurements were performed on ITO/compound/Alq_3/Al device. The azomethine solution (1 w/v% in dichloroethane) was spin-cast onto ITO-covered glass substrate at room temperature. Residual solvent was removed by heating the film in a vacuum. Alq_3 layer was prepared on the polymer film surface by vacuum deposition at a pressure of 10^{-6} Torr and then Al electrode was vacuum deposited at the same pressure. The area of the diodes was 9 mm^2. Current–voltage characteristics were detected using electromether Keithey 6715.

The phase transitions and mesogenicity were studied by differential scanning calorimetry (DSC) and polarizing microscope observations (POM). DSC were measured on a TA-DSC 2010 apparatus using sealed aluminium pans under nitrogen atmosphere at a heating/cooling rate 0.5 °C/min in a temperature range from −20 °C to over the clearing point.

The textures of the liquid-crystalline phase were observed with a Polarized Optical Microscopy (POM), set-up composed of: i) LEICA DMLM Microscope (magnification: 2.5×, 5×, 10×, 20× and 50×) working in both transmission and reflexion modes, ii) LINKAM LTS350 (−196 °C till +350 °C) Hot plate and LINKAM CI94 temperature controller, and iii) JVC Numeric 3-CCD KYF75 camera (resolution: 1360×1024).

2.3. General synthetic procedure of (**1**)–(**4**)

A mixture of aldehyde (1.0 mmol) and amine (1.0 mmol) in N,N-dimethylacetamide (DMA) solution, with the presence of *p*-toluenesulfonic acid (PTS) (0.06 g) was refluxed with stirring for 10 h. The reaction was conducted in an argon atmosphere and the condenser was fitted with a Dean-stark trap. After cooling, the mixture was precipitated with 100 ml of ethanol. The crude product was washed with methanol (500 ml) and next with acetone (350 ml) to remove the unreacted monomers. Then the compound was dried at 60 °C under vacuum for 12 h.

(1): Yield: 90%. FTIR: ν_{max} in cm^{-1} 3031, 2960, 2954, 2918, 2849, 1623 (HC=N–), 1599, 1580, 1559, 1502, 1486, 1467, 1450, 1406, 1363, 1312, 1210, 1179, 1115, 1006, 973, 889, 834, 819, 759, 719, 687, 558, and 533. ^1H NMR (200 MHz, $CDCl_3$, TMS) [ppm]: δ 8.52 (s, 1H, HC=N–); 7.98, 7.95, 7.72, 7.69, 7.67, 7.66, 7.64, 7.47, 7.45, 7.23, 7.21, 7.19, 2.63, 1.63, 1.61, 1.56 (H_2O from $CDCl_3$), 1.27, and 0.88 (as in Fig. 2). ^{13}C NMR (50 MHz, $CDCl_3$, TMS) [ppm]: δ 159.06 (–HC=N–), 140.99, 129.16, 129.11, 128.87, 127.84, 127.41, 127.16, 120.81, 35.51, 31.89, 31.54, 29.61, 29.51, 29.32, 22.67, and 14.10.

(2): Yield: 92%. FTIR: ν_{max} in cm^{-1} 3031, 2954, 2917, 2849, 1624 (HC=N–), 1599, 1580, 1560, 1502, 1465, 1450, 1407, 1364, 1312, 1169, 1115, 1006, 973, 889, 834, 759, and 719. ^1H NMR (200 MHz, $CDCl_3$, TMS) [ppm]: δ 8.52 (s, 1H, HC=N–); 7.98, 7.95, 7.72, 7.69, 7.67, 7.66, 7.64, 7.49, 7.47, 7.45, 7.26, 7.23, 7.21, 7.19, 2.63, 1.59 (H_2O from $CDCl_3$), 1.26, and 0.88 (as in Fig. 2). ^{13}C NMR (50 MHz, $CDCl_3$, TMS) [ppm]: δ 159.09 (–HC=N–), 149.58, 143.85, 141.00, 140.31, 135.31, 130.28, 129.16, 129.12, 129.01, 128.87, 128.46, 127.85, 127.69, 127.41, 127.16, 120.82, 35.51, 35.07, 31.92, 31.83, 31.56, 29.69, 29.60, 29.52, 29.36, 29.31, 22.68, and 14.13.

(3): Yield: 89%. FTIR: ν_{max} in cm^{-1} 3030, 2875, 1628 (HC=N–), 1600, 1505, 1450, 1415, 1370, 1300, 1201, 1172, 1153, 1136, 1104, 1093, 1048, 979, 918, 886, 848, 766, 723, 699, 653, 562, and 529. ^1H NMR (200 MHz, $CDCl_3$, TMS) [ppm]: δ 8.48 (s, 1H, HC=N–); 8.01, 7.97, 7.75, 7.72, 7.68, 7.67, 7.65, 7.64, 7.63, 7.61, 7.31, 7.28, 7.26, and 1.57 (H_2O from $CDCl_3$), (as in Fig. 2). ^{13}C NMR (50 MHz, $CDCl_3$, TMS) [ppm]: δ 161.64 (–HC=N–), 156.28, 144.34, 140.79, 134.60, 129.56, 128.94, 128.07, 127.55, 127.20, and 120.96.

(4): Yield: 82%. FTIR: ν_{max} in cm^{-1} 2881, 2825, 1636 (HC=N–), 1597, 1558, 1516, 1488, 1445, 1403, 1361, 1313, 1299, 1286, 1236, 1149, 1145, 1074, 1007, 946, 889, 821, 762, 736, 723, and 963. ^1H NMR (200 MHz, $CDCl_3$, TMS) [ppm]: δ 8.57 (s, 1H, HC=N–); 8.02, 7.99, 7.93, 7.91, 7.90, 7.87, 7.74, 7.71, 7.68, 7.67, 7.65, 7.48, 7.47, 7.45, 7.41, 7.36, 7.33, 7.25, 6.78, 6.75, 3.09, 3.03, 2.91, 2.80, and 1.57 (H_2O from $CDCl_3$), (as in Fig. 2). ^{13}C NMR (50 MHz, $CDCl_3$, TMS) [ppm]: δ 159.72 (–HC=N–), 131.96, 130.72, 124.82, 124.10, 123.25, 121.53, 114.72, and 111.53.

3. Results and discussion

3.1. Synthesis and characterization

Azomethines described in this paper were prepared from 4-biphenyl carboxaldehyde and four amines via high temperature solution condensation in N,N-dimethylacetamide (DMA) at 160 °C. Chemical structures of the azomethines (abbreviated hereinafter as (**1**)–(**4**)) are presented in Fig. 1.

3.2. NMR study

Their expected chemical constitution is confirmed by spectroscopic studies. In the Experimental section NMR data concerning all imines investigated are collected. In particular the signals in the range of 159–161 ppm, present in the ^{13}C NMR spectra of all compounds, confirm the existence of the azomethine group carbon atoms. The changes in the chemical shift, observed upon the modification of the chemical constitution of the amine originating sub-unit are clearly observed. For example, in the case of (**3**), the presence of fluoro atoms in the chain results in an up-field shift of the line related to the azomethine carbon atom in comparison with another azomethines. On the other hand, the presence of azo group (**4**) induces an up-field shift of the line related to the azomethine carbon atom in comparison with (**3**) and results in a very small down-field shift of the line related to the azomethine carbon atom in comparison with (**1**) and (**2**).

Most signals were assigned based on well-known proton NMR chemical shift displacements resulting from electron shielding/deshielding of the hydrogen nuclei by the inductive effects or from the diamagnetic anisotropy of various neighboring groups. In the Experimental section ^1H NMR data concerning all compounds were investigated while in Fig. 2a ^1H NMR spectra of the imines are present.

In particular in proton NMR spectra of the investigated compounds the azomethine proton signal was observed in the range of 8.48–8.57 ppm as it was expected (Fig. 2). For example, in the imine (**4**) the signal from the imine group at 8.57 ppm was observed and was down-field shift in comparison with another compounds. On the other hand the presence of the azo group in (**3**) caused significant up-field shift of the imine proton signals to 8.48 ppm with respect of the line related to imine proton in comparison with another azomethines (see Experimental section). No chemical shift of the imine group proton and carbon was observed along with an increase in length of the aliphatic chain from 10 to 16 (compare (**1**) and (**2**)).

3.3. FTIR study

The presence of the imine group was also confirmed by FTIR spectroscopy since in each case the band characteristic of the HC=N– stretching deformations was detected. The exact position of this band varies in the spectral range 1624–1636 cm^{-1} shifting towards higher wavenumbers for the compound with the azo group in the structure. Particular bands appearing in FTIR spectra of the imines investigated are shown in the Experimental section. In addition to the –HC=N– stretching band, a band in the range 1597–1600 cm^{-1} can be distinguished to the C=C stretching deformations in the aromatic ring. As an example FTIR spectra of (**1**) and (**3**) are shown in Fig. 2b. Absorption at shorter

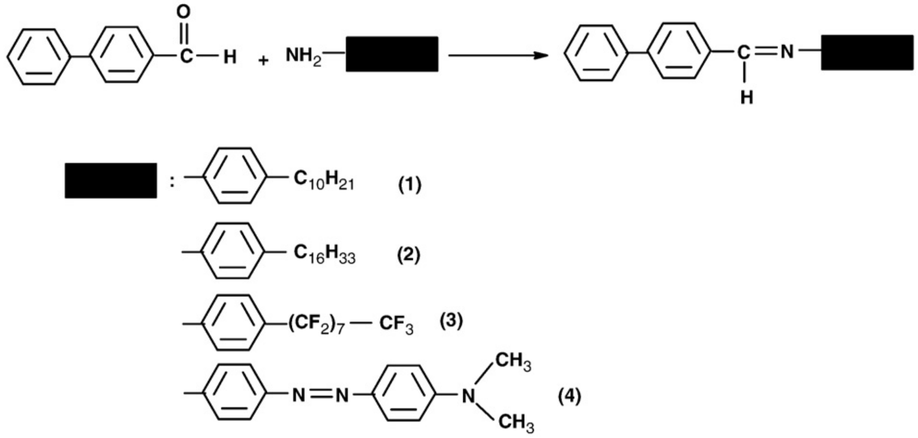

Fig. 1. Synthetic route and chemical structure of the synthesized azomethines.

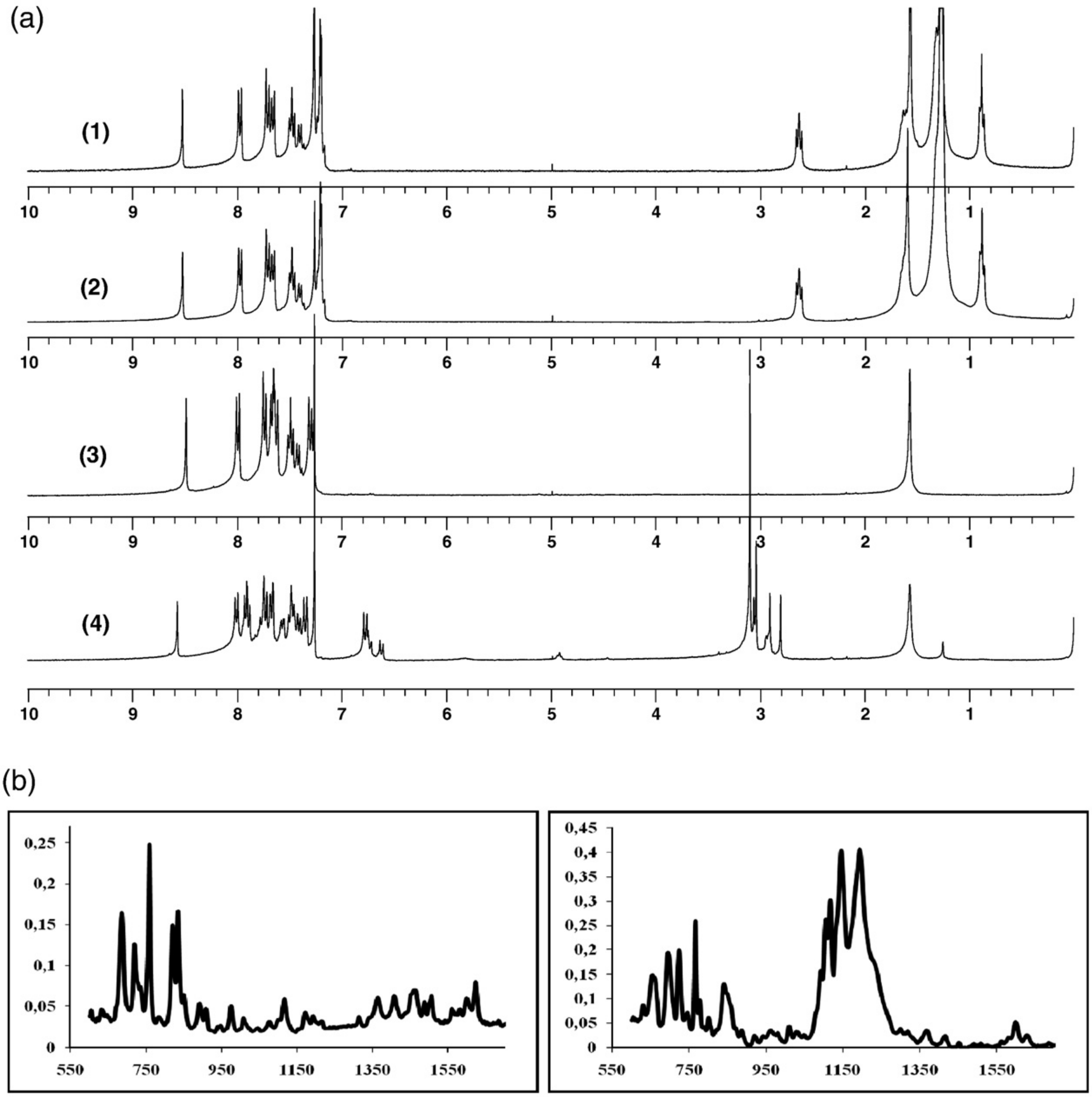

Fig. 2. (a) ^{1}H NMR spectra of all azomethines and (b) FTIR spectra of the azomethines (1) (left side) and (3) (right side) in the range 500–1700 cm^{-1}.

wavelength being in the range of 1623–1624 cm^{-1} was observed for the azomethines (**1**) and (**2**) (see Experimental section). The position of the azometine band is shifting towards higher wavenumbers for the imines (**3**) and (**4**) and shows an intense absorption band at 1628 and 1636 cm^{-1}, respectively. Higher wavenumber value indicates that the bond between carbon and nitrogen atoms in the imine group is shorter that means that the π-electrons in the double bond are less involved in conjugation. The lower wavenumber of the imine group absorption indicates the better conjugation of π-electrons caused by influence of adjusted group to the azomethine linkage.

Table 1
Phase transition temperature (°C) of the compounds detected by POM.

Code	Phase transitions [°C], cooling, POM	Ref.
(**1**)	SmX 124, SmA 129, I	This work
(**2**)	Cr 98, SmX 109, SmA 114, I	This work
(**3**)	Cr 115, SmX 137, SmA 201, I	This work
(**4**)	Cr 160, SmX 165, N 213, I	This work
(**A3**)	Cr 87, SmA 89, I	[23]
(**F2**)	Cr 107, SmC 129, SmA 131, I	[22]
(**F4**)	Cr 115, Sm X1 240, SmA 290, I	[22]

Cr, Sm and I indicate crystal, smectic and isotropic phases, respectively.

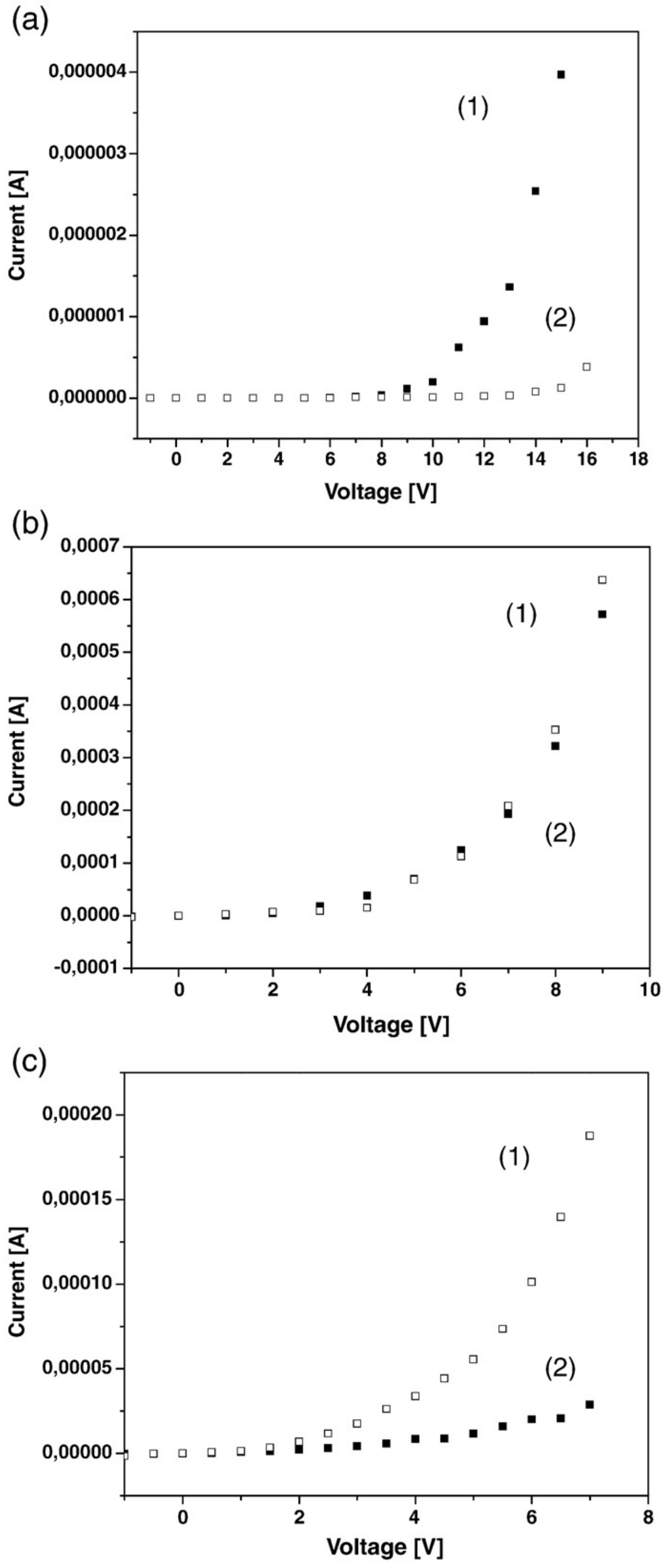

Fig. 3. Current–voltage curves of devices: (a) ITO/(**2**)/$\mathrm{Alq_3}$/Al, (b) ITO/(**3**)/$\mathrm{Alq_3}$/Al and (c) ITO/(**4**)/$\mathrm{Alq_3}$/Al, thickness about 150 nm (curve (2)) and 200 nm (curve (1)).

In accordance with the NMR and FTIR spectra collected in the experimental part the spectral data obtained are in agreement with the spectral data predicted from the chemical formulae of the synthesized compounds.

3.4. Current–voltage experiment

Current–voltage curves of ITO/compound/$\mathrm{Alq_3}$/Al are shown in Fig. 3. It can be seen that current increases with applied voltage increase and less or more depended from thickness of the film being 150 nm and 200 nm. The turn-on voltage of the devices was observed at about 2 V in room temperature for the compound (**4**), at about 4 V for the compound (**3**) and at about 9 V for the compound (**2**) when thickness of the film was 200 nm.

The turn-on voltage of the devices with thickness of the film about 150 nm was observed at about 5 V in room temperature for the compound (**4**), at about 4 V for the compound (**3**) and at about 14 V for the compound (**2**). Value of conductivity of the investigated azomethines (**3**) and (**4**) was about 10^{-7} [S/m], while for the azomethine (**2**) was about 10^{-8} [S/m], what categorized probe materials between semiconductors and dielectrics [35–42].

Different types of conjugated polymers such as poly(acetylene), poly(p-phenylene), poly(p-phenylenevinylene), poly(aniline), poly(pyrrole) and poly(thiophene) have been developed and intensively investigated as organic semiconductors [35–42]. Concerning the electrical properties of the poly(azomethine)s it should be stressed that the conductivities of undoped polymers are low (10^{-16}–10^{-11} S/m), but doping causes an increase of the conductivity even to 10^{-9} S/m [14]. The turn-on voltage of the device (**F2**) was observed at about 6 V

Table 2
Transition temperatures and enthalpies of the azomethines detected by DSC.

Code	Phase transitions [°C] (corresponding enthalpy changes) [J/g], DSC		Ref.
	Heating	Cooling	
(**1**)	78.1 (3.2), 95.0 (96.7), 120.6 (8.5), 125.7 (8.6)	73.1 (92.8), 119.9 (8.6), 124.2 (7.9)	This work
(**2**)	107.1 (113.3), 112.2 (2.8)	105.2 (12.1), 97.2, 96.2 (105.5)	This work
(**3**)	100.1 (0.7), 132.9 (33.9), 192.3 (9.3), 199.8 (1.5)	100.0 (0.5), 111.7 (30.8), 191.2 (8.1), 199.3 (1.4)	This work
(**4**)	54.5 (8.4), 125.8 (4.9), 177.5 (13.5), 236.6 (3.66)	77.3 (1.1), 134.3 (14.1)	This work
(**A3**)	46.8 (6.0), 61.8, (12.1), 87.3 (46.1)	32.1 (4.7), 48.6 (9.9), 85.6 (46.4)	[23]
(**F2**)	108.3 (15.08), 128.9 (2.68), 131.9 (13.00)	106.9 (14.55), 128.7 (2.62), 131.5 (12.70)	[22]
(**F4**)	118.7 (11.17), 202.2 (4.77), 297.4 (8.59)	93.7 (5.58), 200.5 (1.59), 296.9 (8.51)	[22]

in room temperature [22] similar as for poly(azomethine)s with triphenylamine core (PAZ-TPA) in the main chain devices [43]. On the other hand for the azomethine obtained from heptadecafluoroundecyloxy benzaldehyde and pyren-1-amine the turn-on voltage of the device ITO/azomethine/Alq$_3$/Al was observed at about 8 V in room temperature [22].

We found differences between I–V characteristic of the azomethines presented in this paper and azomethines based on heptadecafluoroundecyloxy benzaldehyde [22]. For example, the turn-on voltage of the device (**F2**) was observed at about 6 V in room temperature, while for the azomethine (**2**) was 9 V. This behavior confirmed the influence of the aldehyde used in the synthesis of the azomethines on the electrical properties of the compounds.

3.5. Mesomorphic behavior

Our investigations showed that the all azomethines (**1**)–(**4**) have mesomorphic behavior. All azomethines were studied by differential scanning calorimetry (DSC) and Polarized Optical Microscopy (POM) method to determine their mesomorphic properties. The tentative mesophase identifications and the scenario of phase transitions related to all compounds are based on the identification of textures appearing in two reference textbooks for liquid crystals [44,45] and on repeated POM and DSC experiments.

The POM and DSC observations revealed that all of the compounds were enantiotropic liquid crystals. Azomethines (**1**)–(**3**) exhibited two mesophases such as SmA and SmX (probably SmB). In contrast, the azomethine (**4**) exhibited two totally different mesophases in comparison with (**1**)–(**3**) such as SmX2 (probably SmG) and nematic mesophases, which implies a significant effect of the azo group (N=N) on the mesomorphic properties.

Details of transition temperatures of the compounds as determined by POM are summarized in Table 1 together with their phase variants. The transition temperatures and enthalpies of the azomethines (**1**)–(**4**) determined by DSC are presented in Table 2.

The azomethine (**1**) has an enantiotropic smectic A and X (probably SmB) mesophases. During cooling scans from 129.0 °C to 123.5 °C and during heating scans from 123.8 °C to 130 °C, the development of the typical colorful focal conic fan texture colorful of a SmA mesophase (see Fig. 4a) was observed. Additionally, homeotropically aligned SmA domains of (**1**) were found (Fig. 4a).

Exactly at 123.5 °C during cooling scans a sharp transition consisting in the appearance of transitory (quick appearing and disappearing) bars within the focal–conic fans texture of the SmA mesophase of (**1**) was observed, which unambiguously indicate the transition between a SmA

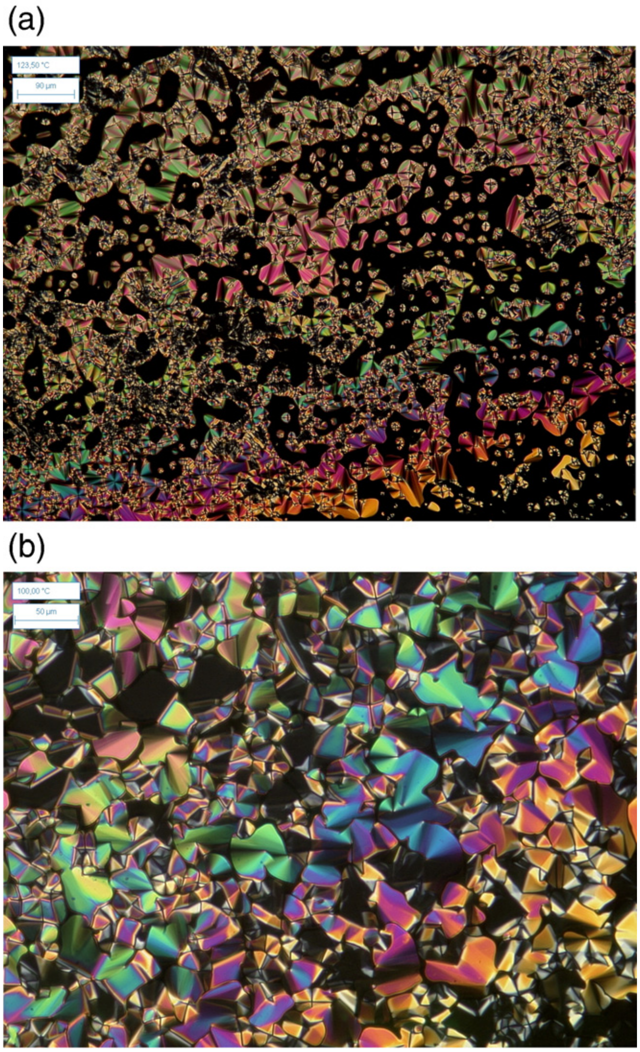

Fig. 4. Photomicrographs of the optical textures of mesophases obtained for (**1**): (a) SmA-focal conic fan and homeotropic alignment area, (seen at 123.5 °C) and (b) SmX mosaic texture and focal conic fan texture (seen at 100 °C).

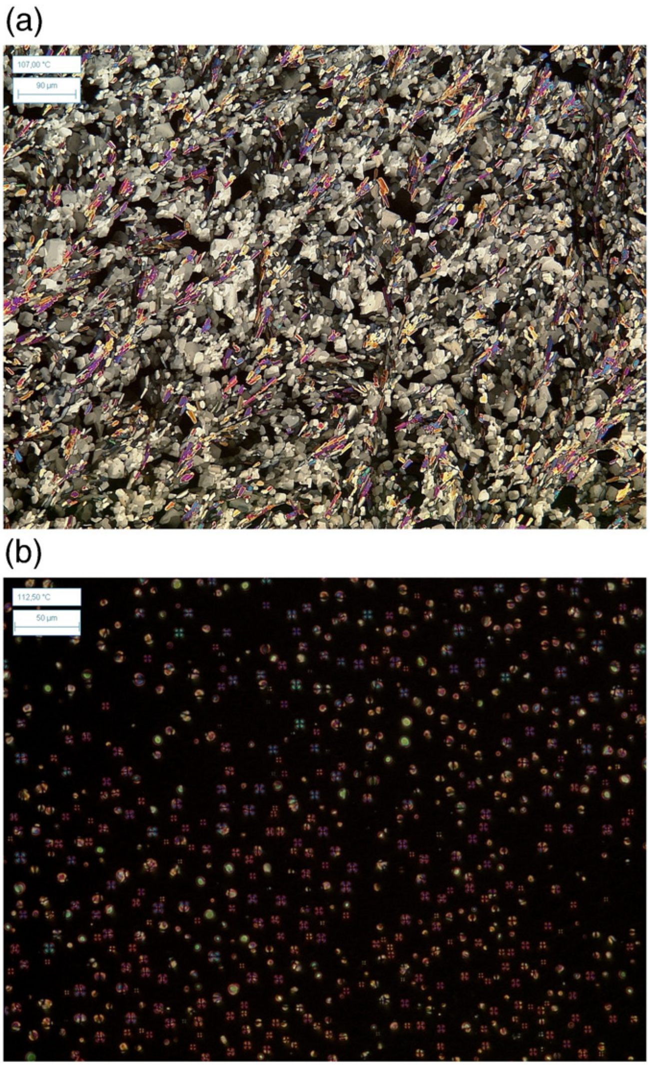

Fig. 5. Photomicrographs of the optical textures of mesophases obtained for (**2**): (a) SmX mosaic texture, (seen at 107 °C) and (b) SmA texture (seen at 112.5 °C).

and a SmX mesophase (Fig. 4b). Indeed, as the arcs, which suddenly appeared within the fan of the SmA mesophase, did not persist below 123 °C in the form of fine or blurred lines. Also a homeotropically aligned SmX (probably SmB) mesophase of (**1**) can also (as a SmA) give a black POM image. Additionally, by cooling the sample slowly enough to develop its SmX mesophase under 123 °C it was possible to obtain

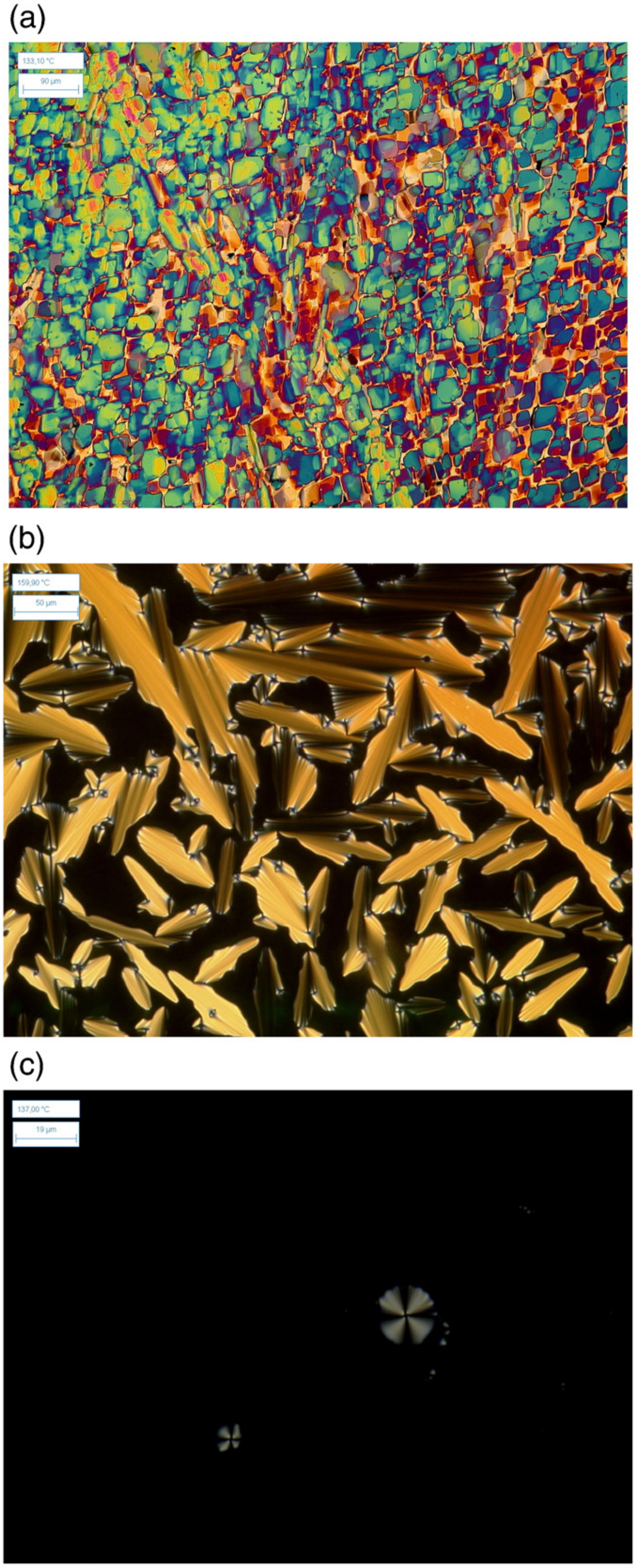

Fig. 6. Photomicrographs of the optical textures of mesophases obtained for (**3**): (a) SmX —colored mosaic with rectangular platelets, (seen at 133.1 °C), (b) SmA— conic focal fan and homeotropic alignment area, (seen at 159.9 °C) and (c) SmA— homeotropic alignment area with two defects, (seen at 137 °C).

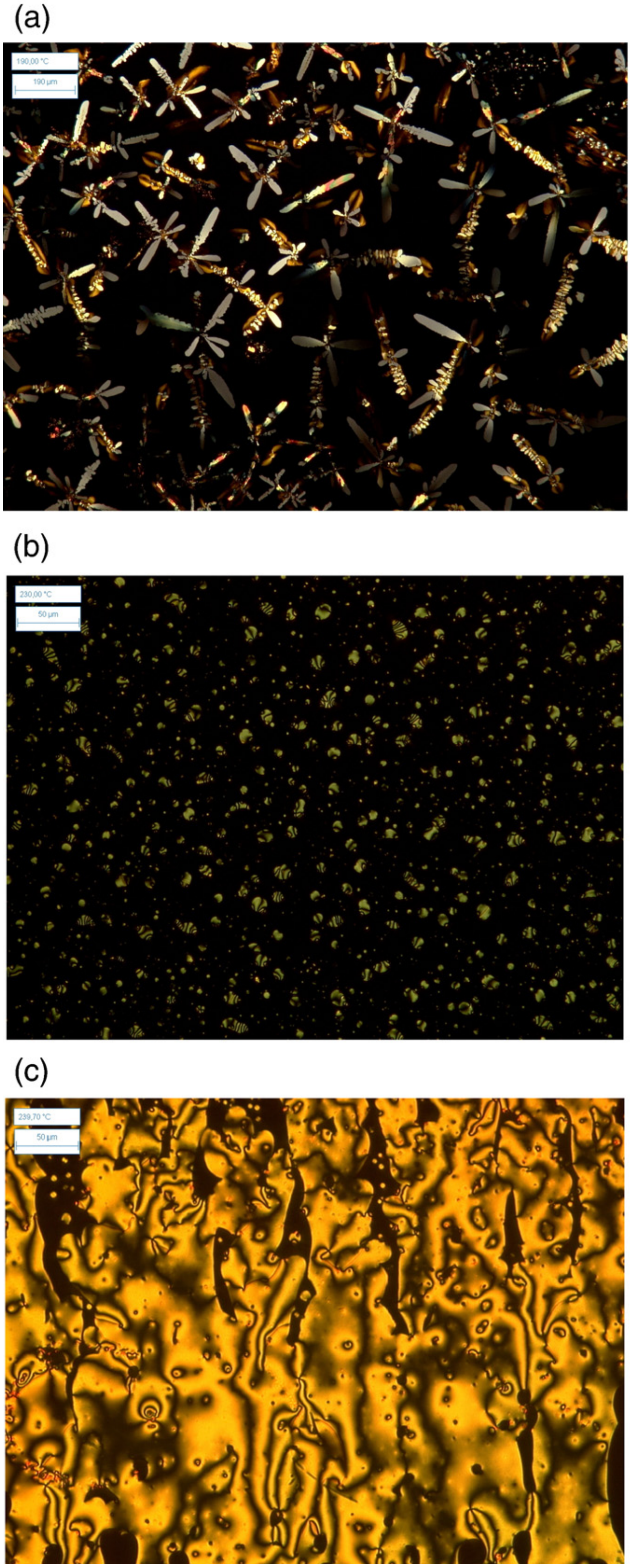

Fig. 7. Photomicrographs of the optical textures of mesophases obtained for (**4**): (a) SmX2 —dendritic growth of mosaic texture and splinters, (seen at 190 °C), (b) nematic droplets and small schliren, (seen at 230 °C) and (c) nematic Schliren, (seen at 239.7 °C).

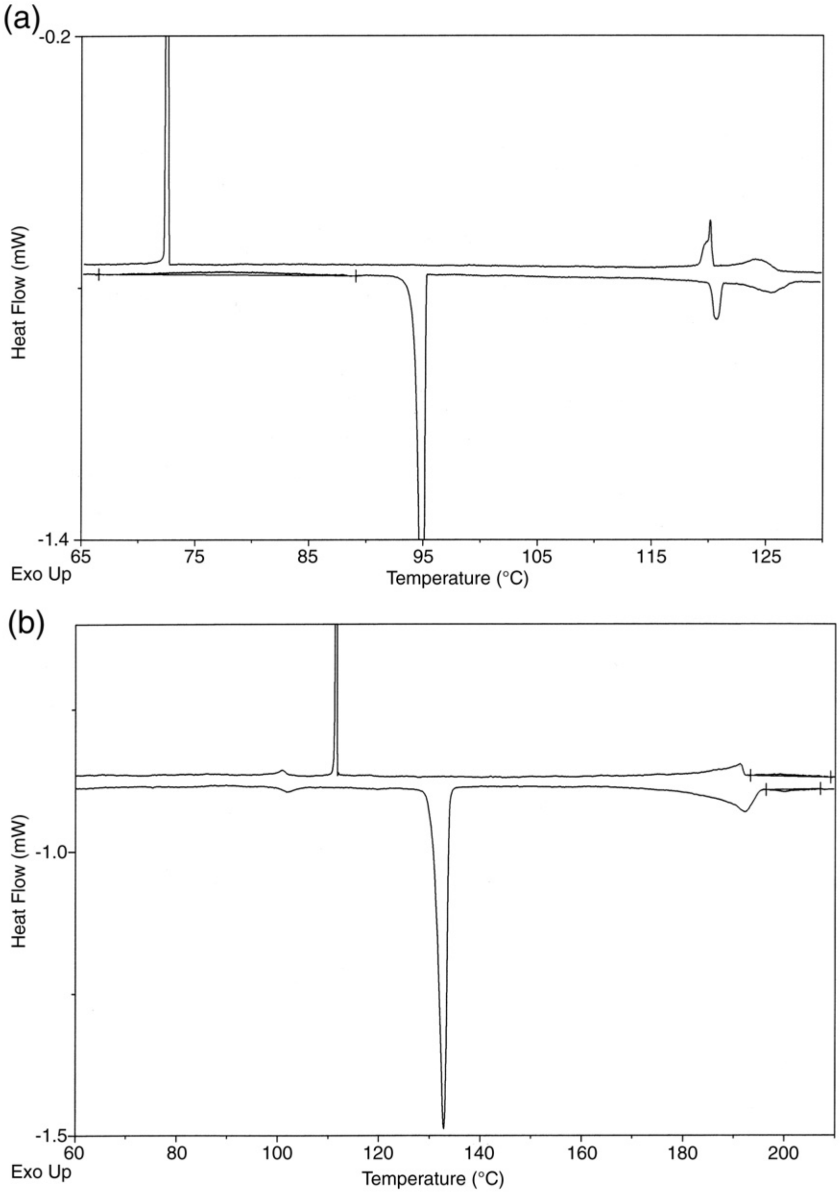

Fig. 8. DSC traces of the: (a) azomethine (**1**) and (b) azomethine (**3**) obtained on the second heating and cooling, under N_2 atmosphere.

colorful POM picture in which the mosaic and focal–conic fan textures were simultaneously present (Fig. 4b).

For the azomethine (**2**) all transitions detected by POM were in good agreement with the DSC analyses. SmA mesophase showed a 2D (lamellar) organization (with orientational order but no positional order within a layer). On the other hand more ordered X-type mesophase could lead to two closely related SmB mesophases which show the same POM textures and that can only be distinguished by X-ray diffraction. In the above-mentioned proposed scenario of phase transitions, we just indicated that the second mesophase observed on cooling from the isotropisation state was a SmX (probably SmB) (Fig. 5a).

The SmA mesophase of (**2**) exhibited a black texture (homeotropically aligned SmA mesophase) perturbed by a myriad of small and colorful defects (leaf-like and small fan-like) which reflect areas of the POM sample which are in a conventional SmA planar texture (see Fig. 5b).

The fact that the azomethine (**3**) has perfluorinated tails is considerably increasing the stability of the SmA mesophase of this LC, allowing a clearing point of ca. 203 °C. Concomitantly, the perfluorinated tails of (**3**) molecules are driving the texture of SmA mesophase almost exclusively to the homeotropic one. It was not a surprise for us that, the temperature at which the SmA is transformed to SmX (probably SmB) transition occurred for (**1**) and (**3**) at 123.0 °C and 136.0–137.0 °C, respectively what confirmed the replacement of n-$C_{10}H_{21}$ (**1**) by n-C_8F_{17} (**3**). During cooling scans from 203.0 °C to 136.0–137.0 °C and during heating scans from 136.0–137.0 °C to 202.0 °C the development of the typical colorful focal conic fan texture of a SmA mesophase (see Fig. 6b) was observed. Moreover, homeotropically aligned SmA areas with 2 focal conic fan defects were found (Fig. 6c). Contrary to (**1**), for (**3**) we did not observed a sharp transition consisting in the appearance of transitory bars within the focal–conic fans texture of the SmA mesophase of (**1**) which could have unambiguously indicated the transition in between a SmA and a SmX (probably SmB) mesophase. Indeed, careful and slow heating of a crystallized (**3**) sample over its melting point (118 °C) allowed us to image mosaic texture (with some rectangular-like platelets) of its SmX mesophase from 133 °C onwards (see Fig. 6a).

The azomethine (**4**) has two enantiotropic mesophases such as SmX2 (probably SmG) and N. Transitions observed by POM are in very good agreement with the DSC analyses. Unfortunately, the compound (**4**) was

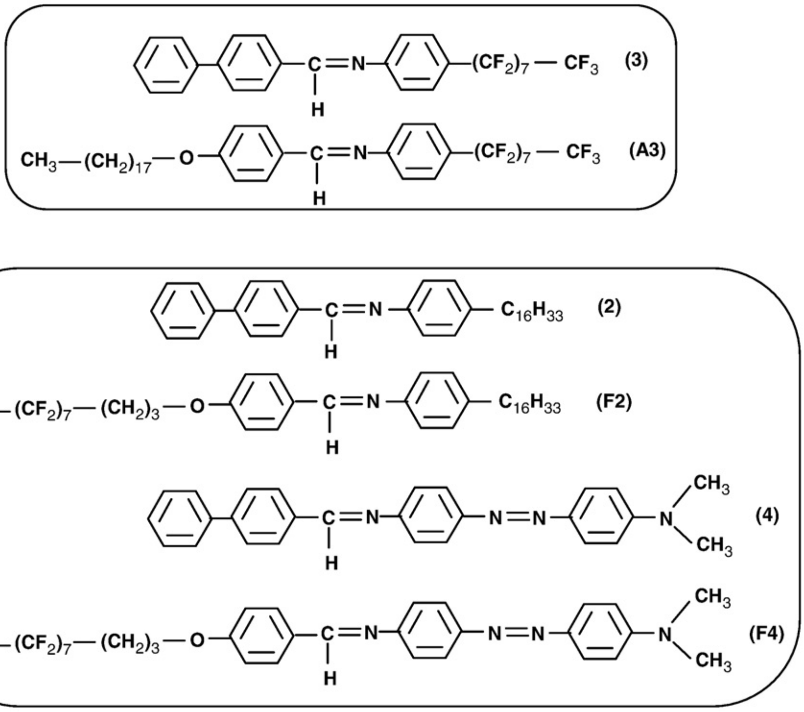

Fig. 9. Chemical structure of the selected azomethines with different types of side groups.

simultaneously going to its isotropic state and is partly decomposed. It is very difficult during POM experiments to accurately determine the clearing point of this LCs. Moreover vapor phase transport of this deeply yellow/orange compounds on the windows of hot plate at temperature higher than 250 °C prevents an easy determination of the clearing point. The observed nematic (droplet, Schlieren, thread-like) textures of (**4**) (Fig. 7b–c) were strongly destabilized (without completely disappearing) at a temperature of ca. 260 °C, but this does not mean that the transition of the N to isotropisation occurred at this temperature. During cooling scans from 265–270 °C to 200 °C–195 °C and during heating scans from 212.5 °C to 260 °C, the development of colorful and quickly moving birefringent textures was observed that can be related to nematic mesophases such as droplet texture, Schlieren texture, droplet and small Schlieren textures and Schlieren and thread-like texture (see Fig. 7b–c). When looking at the molecular structure of (**4**), it is no surprise that this rod-like mesogen is giving rise to a nematic mesophase. Nevertheless, the fact that it contains an azo group (which can quickly isomerize at high temperature under white-light illumination) can explain why it was quite difficult to get nice POM images. Shape fluctuation and modification of shape-persistency could be the reason for the difficulty we encountered to capture good POM images of this N mesophase over large area. During cooling scans from 200–195 °C to 165–155 °C and during heating scans from 170 °C to 210 °C, the developments of very peculiar birefringent textures that can be related to a SmX2 (probably SmG) mesophase were found: (a) dendritic growth of a mosaic texture if which elongated platelets with side-splinters are merging from black (homeotropically aligned) domains and (b) mosaic texture (see Fig. 7a). It is quite difficult to differentiate a SmB mesophase from a SmG mesophase based solely on the observation of their textures by POM as the latter mesophase is a titled version of the former one. Nevertheless few tips are suggesting that the mesophase appearing below the N one of (**4**) during cooling scans is indeed a SmG one. The fact that we were able to image the dendritic growth of a mosaic texture in which elongated platelets with side-splinters are emerging from black (homeotropically aligned) domains is strongly in favour of its attribution to a SmG mesophase.

DSC thermograms of the azomethines (**1**) and (**3**) obtained on the second heating and the second cooling, under N_2 atmosphere are shown in Fig. 8, as examples.

Tables 1–2 reveal that the compounds (**3**)–(**4**) exhibited a clearing point temperature higher than 200 °C and broad thermal range of the mesophase. For example, the thermal range of SmX phase of the compound (**3**) exceeds 64 °C and the SmX2 mesophase of the azomethine (**4**) exceeds 48 °C (see Table 1). On the other hand the compounds (**1**) and (**2**) have a clearing point temperature at about 120 °C and narrow thermal range of the mesophase (see Table 1). This behavior indicates the role of the side chain in creating their mesomorphic properties.

Because in our previous work we investigate azomethines obtained from different aldehydes ((**A3**), (**F2**), and (**F4**)) and the same amines [22,23] we have possibility to compare few of them and show not only influence of amine but also aldehyde on the mesomorphic properties of the compounds. For these reason we presented on Fig. 9 the structure of the responsible azomethines, while in Tables 1 and 2 we presented the thermal characteristic of the compounds.

Considering the temperature of isotropisation the following scenario was observed: 86 °C (**A3**) > 199 °C (**3**), 96 °C (**2**) > 132 °C (**F2**) and 134 °C (**4**) > 297 °C (**F4**). It was not a surprise that the introduction of the long aliphatic chain as in the case of (**A3**) influenced the decrease of the temperature of isotropisation in comparison with (**3**). Contrary, the presence of alkoxysemiperfluorinated chain as in the case of (**F2**) and (**F4**) influence the increase of the temperature of isotropisation (compare (**2**) and (**F2**) and (**4**) and (**F4**)). Different aldehydes used in the synthesis of the azomethines influence also on the kind of mesophase (Table **1**). Compound (**A3**) obtained from 4-octadecyloxybenzaldehyde exhibited only SmA mesophase while (**3**) has additionally SmA and also SmX mesophase. For (**F2**) two mesophases such as SmA and SmC were found while for the azomethine (**2**) instead SmC mesophase SmX was observed. Totally different kinds of mesophases were found for (**4**) and (**F4**) (Table 1). This behavior could be explained by the fact that in (**F4**) additionally to azo bond there exists also alkoxysemiperfluorinated chain (Fig. 9).

4. Conclusion

In summary, we prepared a series of liquid-crystalline unsymmetrical azomethines by the condensation of 4-biphenyl carboxaldehyde with aliphatic and aromatic amines. The thermal properties of these compounds were investigated via DSC and POM techniques. All azomethines showed the smectic mesomorphism. The mesophases of the azomethines (**1**)–(**3**) were designated to be SmA and SmX phases. Azomethine (**4**) showed smectic X2 and N phases. Preliminary investigations of the current–voltage characteristics for device such as ITO/azomethine/Alq_3/Al confirmed their semiconductivity properties of the organic thin film and showed that the thickness of the film influences less or more for the electrical properties of the investigated compounds.

References

[1] M. Hird, Chem. Soc. Rev. 36 (2007) 2070.
[2] J.M. Frechet, Prog. Polym. Sci. 30 (2005) 844.
[3] C. Tschierske, Chem. Soc. Rev. 36 (2007) 1930.
[4] C.T. Imrie, P.A. Henderson, Chem. Soc. Rev. 36 (2007) 2096.
[5] J. Barbera, B. Donnio, L. Gehringer, D. Guillon, M. Marcos, A. Omenat, J.L. Serrano, J. Mater. Chem. 15 (2005) 4093.
[6] D. Demus, Liquid Cryst. 5 (1989) 75.
[7] W. Ong, R.L. McCarley, Org. Lett. 7 (2005) 1287.
[8] A.G. Cook, U. Baumeister, C. Tschierske, J. Mater. Chem. 15 (2005) 1708.
[9] B. Donnio, S. Buathong, I. Bury, D. Guillon, Chem. Soc. Rev. 36 (2007) 1495.
[10] M. Marcos, R.M. Rapun, A. Omenat, J.L. Serrano, Chem. Soc. Rev. 36 (2007) 1889.
[11] I.M. Saez, J.W. Goodby, J. Mater. Chem. 15 (2005) 26.
[12] V. Percec, Phil. Trans. R. Soc. A 364 (2006) 2709.
[13] V. Percec, M.R. Imam, M. Peterca, D.A. Wilson, R. Graf, H.W. Spiess, V.S.K. Balagurusamy, P.A. Heiney, J. Am. Chem. Soc. 131 (2009) 7662.
[14] A. Iwan, D. Sek, Prog. Polym. Sci. 33 (2008) 289.
[15] J.A. Smith, R.A. DiStasio, N.A. Hannah, R.W. Winter, T.J.R. Weakley, G.L. Gard, S.B. Rananavare, J. Phys Chem B. 108 (2004) 19940.
[16] I.K. Grabtchev, V.B. Bojinov, I.T. Moneva, J. Mol. Struct. 471 (1998) 19.
[17] H. Hioki, M. Fukutaka, H. Takahashi, M. Kubo, K. Matsushita, M. Kodama, K. Kubo, K. Ideta, A. Mori, Tetrahedron 61 (2005) 10643.
[18] T. Narasimhaswamy, K.S.V. Srinivasan, Liquid Cryst. 31 (2004) 1457.
[19] C.V. Yelamaggad, I.S. Shashikala, G. Liao, D.S.S. Rao, S.K. Prasad, Q. Li, A. Jakli, Chem. Mater. 18 (2006) 6100.
[20] O. Stamatoiu, A. Bubnov, I. Tarcomnicu, M. Iovu, J. Mol. Struct. 886 (2008) 187.
[21] J. Godzwon, M.J. Sienkowska, Z. Galewski, J. Mol. Struct. 844–845 (2008) 259.
[22] A. Iwan, H. Janeczek, B. Jarzabek, M. Domanski, P. Rannou, *Liq. Cryst.* 36 (2009) 873.
[23] A. Iwan, H. Janeczek, Mol. Cryst Liq. Cryst. (in press).
[24] D. Ribera, A. Mantecon, A. Serra, Macromol. Chem. Phys. 202 (2001) 1658.
[25] D. Ribera, A. Mantecon, A. Serra, J. Polym. Sci. Part A: Polym. Chem. 40 (2002) 4344.
[26] P.A. Henderson, C.T. Imrie, Macromolecules 38 (2005) 3307.
[27] K. Kishikawa, N. Muramatsu, S. Kohmoto, K. Yamaguchi, M. Yamamoto, Chem. Mater. 15 (2003) 3443.
[28] Y. Naito, R. Ishige, M. Itoh, M. Tokita, J. Watanabe, Chem. Lett. 37 (2008) 880.
[29] S. Sudhakar, T. Narasimhaswamy, K.S.V. Srinivasan, Liquid Cryst. 27 (2000) 1525.
[30] V. Cozan, M. Gaspar, E. Butuc, A. Stoleriu, Eur. Polym. J. 37 (2001) 1.
[31] K. Sabdham, V. Srinivasan, T. Padmavathy, Macromol. Symp. 199 (2003) 277.
[32] A. Iwan, H. Janeczek, P. Rannou, Spectrochim. Acta Part A: Mol. Biomol. Spectrosc. 72 (2009) 72.
[33] A. Iwan, H. Janeczek, B. Jarzabek, P. Rannou, Materials, Special Issue of Liquid Crystals 2 (2009) 38.
[34] A. Iwan, H. Janeczek, P. Rannou, R. Kwiatkowski, J. Mol. Liq. 148 (2009) 77.
[35] A. Pron, P. Rannou, Prog. Polym. Sci. 27 (2002) 135.
[36] M. O'Neil, S.M. Kelly, Adv. Mater. 15 (2003) 1135.
[37] U. Mitschke, P. Bauerle, J. Mater. Chem. 10 (2000) 1471.
[38] H. Shirakawa, E.J. Louis, A.G. Mac-Diarmid, C.K. Chiang, A. Hegger, J. Chem. Soc. Chem. Commun. 16 (1977) 578.
[39] K.Y. Jen, G.C. Miller, R.L. Elsenbaumer, J. Chem. Soc., Chem. Commun. 17 (1986) 1346.
[40] R.L. Elsenbaumer, K.Y. Jen, R. Oboodi, Synth. Met. 15 (1986) 169.
[41] Y. Elsworth, R. Howe, G.R. Isaak, C.P. McLeod, R. New, Nature (1990) 536.
[42] Y. Cao, P. Smith, A.J. Heeger, Synth. Met. 48 (1992) 91.
[43] D. Sek, A. Iwan, B. Jarzabek, B. Kaczmarczyk, J. Kasperczyk, Z. Mazurak, M. Domanski, K. Karon, M. Lapkowski, Macromolecules 41 (2008) 6653.
[44] D. Demus, L. Richter, Textures of Liquid Crystals, 1st Ed, Verlag Chemie, Leipzig, 1978, p. 1.
[45] G.W. Gray, J.W. Gooby, Smectic Liquid Crystals—Textures and Structures, Leonard Hill, Glasgow, 1984, p. 1, and Londow.